One-Pot Synthesis and Surface Modification of Lauric-Acid-Capped $CoFe_2O_4$ Nanoparticles

Yun Teng and Philip W. T. Pong

Department of Electrical and Electronic Engineering, The University of Hong Kong, Hong Kong

This paper presents a facile one-pot method to synthesize monodisperse lauric-acid-capped cobalt ferrite nanoparticles ($CoFe_2O_4$ NPs)and investigates their potential application as drug carriers for loading and controlled release of doxorubicin (DOX). The lauric-acid-capped $CoFe_2O_4$ NPs with a particle size of 15.3 ± 1.7 nm were synthesized via one-pot reaction. Water-soluble lauric-acid-capped $CoFe_2O_4$ NPs were obtained through surface modification with cetyltrimethylammonium bromide (CTAB) and sodium dodecyl sulfate (SDS). Furthermore, the performance of water-soluble lauric-acid-capped $CoFe_2O_4$ NPs for drug delivery was investigated with DOX hydrochloride. The DOX release percentages of CTAB and SDS modified lauric-acid-capped $CoFe_2O_4$ NPs are 56.1% and 48.2%, respectively. These results indicated that the modified lauric-acid-capped $CoFe_2O_4$ NPs could be utilized as a promising candidate for cancer chemotherapy by making use of their pH-sensitive drug-release properties.

Index Terms—**Drug delivery, inverse spinel cobalt ferrite ($CoFe_2O_4$), one-pot method, surface modification.**

I. Introduction

MAGNETIC nanoparticles (NPs) of ferrites have a wide range of applications owing to their particular physicochemical properties and large surface to volume ratio [1], [2], which are different from the bulk materials. The inverse spinel cobalt ferrite ($CoFe_2O_4$) has attracted enormous attention because they have high intrinsic magnetocrystalline anisotropy and large coercivity [3], [4], which can cause a higher heat dissipation than other ferrite NPs with similar size [5]. Thus, they can be used to induce magnetic hyperthermia for various applications [6]–[8]. Several synthesis methods of $CoFe_2O_4$ NPs have been reported previously [9]–[12]. For example, the coprecipitation method has been widely used because of its easy operation and high yield [13]. However, the reported methods involve multiple-step syntheses which are more complicated and time-consuming to obtain the desired resulting NPs. Therefore, producing $CoFe_2O_4$ NPs with an efficient and facile route is still challenging and greatly desired. Typically, the hydrophobic organic ligands (such as oleic acid) coated on the surfaces of the nanocrystalline structures [14] limit the range of biomedical applications of these NPs by making them difficult to disperse in water. The surface modification of CoFe2O4 NPs through surfactant addition and surfactant exchange can improve their water solubility [15], [16]. This is of great importance for their future biomedical applications [17], [18], such as drug delivery which inquires great water solubility of NPs.

In this paper, a facile one-pot method was developed for the synthesis of lauric-acid-capped $CoFe_2O_4$ NPs with promising stability and uniformity, and the NPs were further transferred into aqueous phase through surface modification using surfactants including cetyltrimethylammonium bromide (CTAB) and sodium dodecyl sulfate (SDS). These water-soluble $CoFe_2O_4$ NPs can be directly functionalized with target biomolecules to be applied in an aqueous environment for biosensing, protein separation, and drug delivery [19]–[21]. Finally, the modified lauric-acid-capped $CoFe_2O_4$ NPs were applied to loading and *in vitro* controlled release of doxorubicin (DOX) hydrochloride. This system shows great promise for biomedical applications, especially for targeted cancer therapy.

Manuscript received March 16, 2018; revised April 16, 2018; accepted April 24, 2018. Date of publication May 30, 2018; date of current version October 17, 2018. Corresponding author: P. W. T. Pong (e-mail: ppong@eee.hku.hk).

Color versions of one or more of the figures in this paper are available online at http://ieeexplore.ieee.org.

Digital Object Identifier 10.1109/TMAG.2018.2834524

II. Experiment

A. Materials

The synthesis was carried out using commercially available reagents. Cyclohexene, phenyl oleylamine (>70%), CTAB, sodium ether (99%), 1, 2-tetradecanediol (97%), oleic acid (90%), dodecyl sulfate (SDS), phosphate buffer saline (PBS), and DOX hydrochloride were purchased from Aldrich Chemical Co., Milwaukee, WI, USA. Lauric acid was purchased from Sigma-Aldrich Fine Chemicals, St. Louis, MO, USA. Iron (III) acetylacetonate and cobalt (II) acetylacetonate were purchased from Acros. They were used as received without any further purification. Distilled deionized water was used for the experiment in aqueous solutions. All the chemicals were used as received.

B. Synthesis of Lauric-Acid-Capped $CoFe_2O_4$ Nanoparticles

The monodisperse lauric-acid-capped $CoFe_2O_4$ NPs were synthesized via one-pot reaction following the literature protocol, as shown in Fig. 1 [22]. $Co(acac)_2$ (1 mmol), $Fe(acac)_3$ (2 mmol), 1, 2-tetradecanediol (10 mmol), oleic acid (6 mmol), oleylamine (6 mmol), and phenyl ether (20 mL) were mixed with lauric acid (6 mmol), and the mixture was magnetically stirred under nitrogen. The mixture was heated to 200 °C for 1.5 h and then heated to reflux at 280 °C for 1 h. After cooled to room temperature by removing the heating source, the mixture was purified by precipitating and dissolving operations using acetone and chloroform solvent for several times to remove excessive surfactants. The products were dissolved in 12 mL cyclohexene for further use.

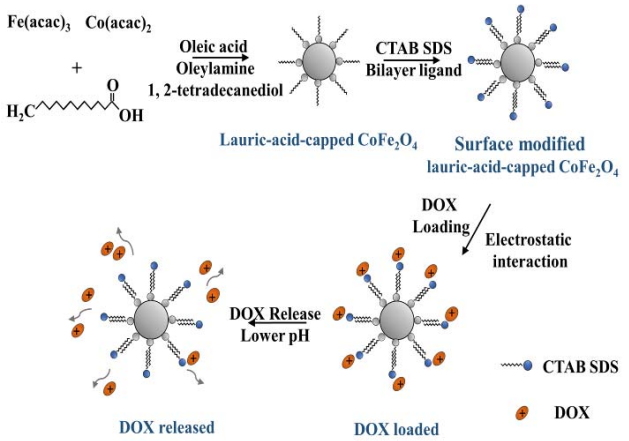

Fig. 1. Schematic of synthesis process for lauric-acid-capped $CoFe_2O_4$ NPs and DOX loading and releasing processes.

C. Surface Modification of Lauric-Acid-Capped $CoFe_2O_4$ Nanoparticles

The as-synthesized lauric-acid-capped $CoFe_2O_4$ NPs were transferred to water using CTAB and SDS, respectively, following the protocol developed in [23]. A 0.5 g of lauric-acid-capped $CoFe_2O_4$ NPs were added to a suspension of CTAB and SDS in deionized water with the concentration of 10 $mg \cdot mL^{-1}$, respectively, and the mixture was stirred for 2 h at 75 °C to obtain a modified water-based $CoFe_2O_4$ solution. Finally, the precipitate was collected by centrifugation and washed with deionized water for several times. The particles were redispersed in 6 mL deionized water.

D. DOX Loading and Release Test of Surface-Modified Lauric-Acid-Capped $CoFe_2O_4$ Nanoparticles

The drug-loading performance of water-soluble lauric-acid-capped $CoFe_2O_4$ NPs was characterized. A 0.03 mg of surface-modified lauric-acid-capped $CoFe_2O_4$ NPs were dispersed in 5 mL of the DOX diluted in ultra-pure PBS at 25 °C (concentration is 0.5 $mg \cdot mL^{-1}$), and the solution was shaken for 24 h. Finally, the modified lauric-acid-capped $CoFe_2O_4$ NPs loaded with DOX were collected by centrifugation. The supernatant was analyzed by UV–Vis spectrophotometer measurement. The *in vitro* drug delivery test was carried out with different pH values at 37 °C. Typically, 5 mg of DOX-loaded lauric-acid-capped $CoFe_2O_4$ NPs were dipped into 10 mL and pH = 4 and 7.4 phosphoric acidic buffer solutions (PBS), respectively. At selected time intervals, the same colume solution was taken and immediately replaced with an equal volume of fresh PBS. The amount of released DOX in the taken PBS was determined using UV–Vis spectrophotometer at 480 nm.

E. Structural and Magnetic Characterization

The morphology and structure of the $CoFe_2O_4$ NPs were analyzed using a Philips CM-100 transmission electron microscope (TEM) operated at 100 kV. X-ray powder diffraction patterns of the NPs were collected on a Brukerc D8-Advance X-ray diffractometer (XRD) with Cu Kα radiation ($\lambda = 1.5418$ Å). The zeta-potential measurements were conducted on a Zetasizer Nano ZS instrument (Malvern Instruments, Malvern, U.K). The surface modified and bare $CoFe_2O_4$ NPs were characterized by a Shimadzu Fourier transform infrared (FTIR)-8300 spectrometer. Magnetization curve measurements were carried out on a MicroSense vibrating sample magnetometer (VSM). The DOX loading and *in vitro* controlled release test were measured by UV spectrometer (Agilent Cary 60) at 480 nm.

III. Results and Discussion

A. Synthesis of Lauric-Acid-Capped $CoFe_2O_4$ Nanoparticles

Morphology of lauric-acid-capped $CoFe_2O_4$ NPs was studied using TEM. The resulting $CoFe_2O_4$ NPs possessed an average size of 15.3 nm with a standard deviation of 1.7 nm, as shown in Fig. 2(a). The NPs can be slightly dissolved in water due to the use of lauric acid as surfactant (solubility in water = 55 mg/L at 20 °C). Crystal structures of the lauric-acid-capped $CoFe_2O_4$ NPs were identified by XRD, as shown in Fig. 2(b). The positions and intensities of the diffraction peaks coincide with the standard diffraction data of inverse spinel structured $CoFe_2O_4$.

The VSM was used to investigate the magnetic properties of the lauric-acid-capped $CoFe_2O_4$ NPs. The hysteresis loop of the lauric-acid-capped $CoFe_2O_4$ NPs is shown in Fig. 2(c); the saturation magnetization (M_s) of the as-synthesized NPs is 72 $emu \cdot g^{-1}$ which is smaller than the value of $CoFe_2O_4$ bulk material (94 $emu \cdot g^{-1}$) [24]. The coercivity of the $CoFe_2O_4$ is around 185 Oe, which is much larger than that of Fe_2O_3 NPs. This indicates that the magnetic anisotropy of the $CoFe_2O_4$ materials has been significantly improved because the Co cation is incorporated into the FeO matrix.

The dispersion behavior of the lauric-acid-capped $CoFe_2O_4$ NPs in water was investigated by observing the stability of NP suspension in aqueous medium, and the stability of the suspension sustained even after 48 h. The stable suspension of the $CoFe_2O_4$ NPs indicates the existence of the hydrogen bond between the aqueous solution and the lauric-acid layer. The aqueous solubility of the lauric-acid-capped $CoFe_2O_4$ NPs makes them an ideal candidate for various *in vivo* biomedical applications like cancer treatment [6].

B. Surface Modification of Lauric-Acid-Capped $CoFe_2O_4$ Nanoparticles

The surface modification process is illustrated in Fig. 1; the lauric-acid molecules can anchor on the $CoFe_2O_4$ NP surface through hydrogen bonds. The lauric-acid-capped $CoFe_2O_4$ NPs with great water solubility were achieved through surface modification with different surfactants, which has both nonpolar and polar groups, while the nonpolar groups bind with the lauric acid layer through strong van der Waals interactions, the polar groups can improve the dispersity of NPs in water. The TEM images of CTAB-and SDS-modified $CoFe_2O_4$ NPs are presented in Fig. 3(a) and (b). The modified $CoFe_2O_4$ NPs exhibit better uniformity and stability than bare NPs, indicating that surface modification is an effective strategy for

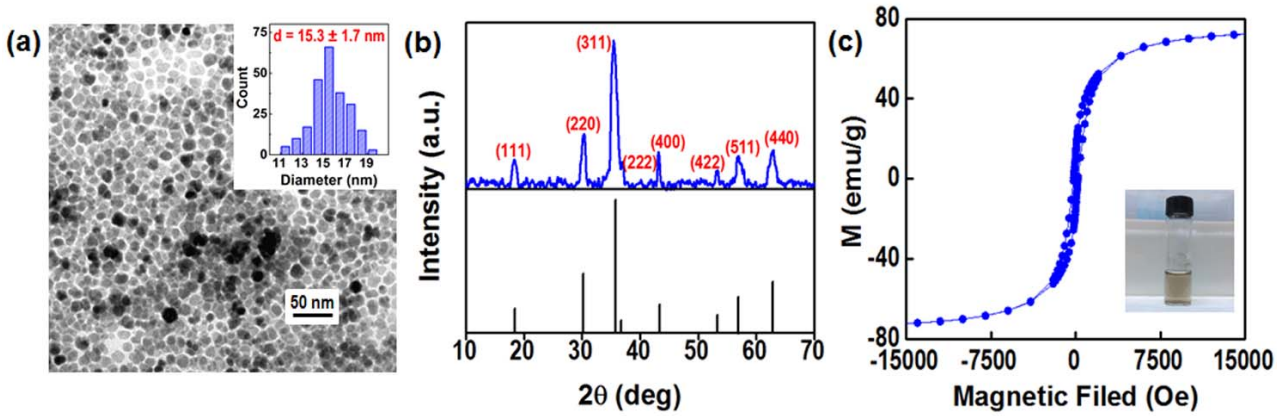

Fig. 2. (a) TEM image of lauric-acid-capped $CoFe_2O_4$ NPs (inset: histogram of particle size). (b) XRD patterns of lauric-acid-capped $CoFe_2O_4$ NPs. (c) Hysteresis loops at 300 K of lauric-acid-capped $CoFe_2O_4$ NPs (inset: stable NPs in aqueous solution).

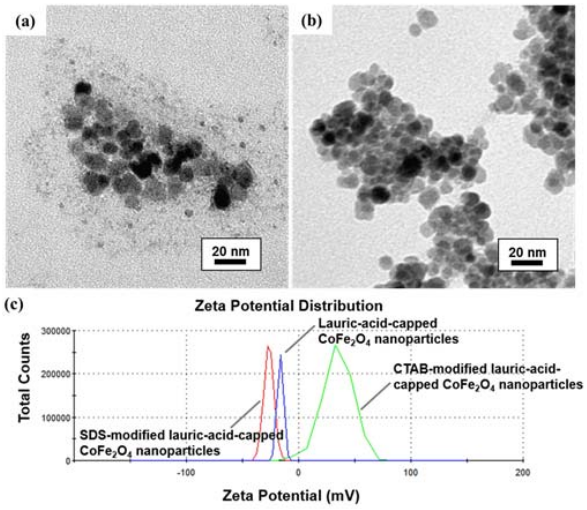

Fig. 3. (a) TEM image of CTAB-modified lauric-acid-capped $CoFe_2O_4$ NPs. (b) TEM image of SDS-modified lauric-acid-capped $CoFe_2O_4$ NPs. (c) Zeta potential of CTAB-and SDS-modified lauric-acid-capped $CoFe_2O_4$ NPs.

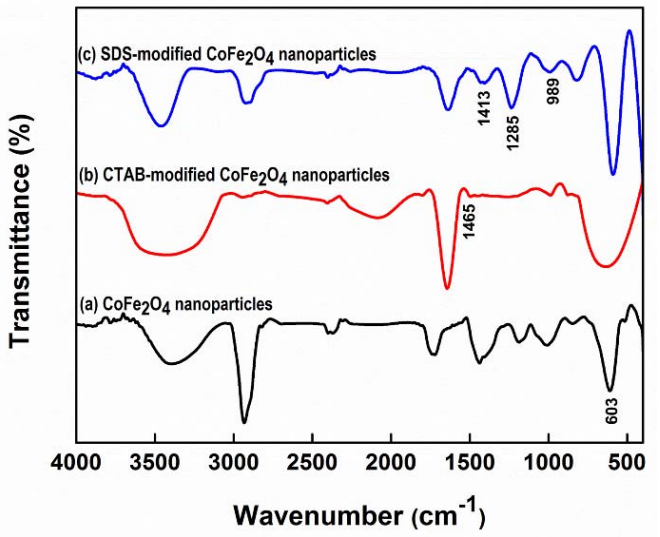

Fig. 4. FTIR of (a) as-synthesized lauric-acid-capped $CoFe_2O_4$ NPs, (b) CTAB-modified lauric-acid-capped $CoFe_2O_4$ NPs, and (c) SDS-modified lauric-acid-capped $CoFe_2O_4$ NPs.

phase transfer of $CoFe_2O_4$ NPs. The stability and interparticle electrostatic interactions of the NPs were determined by the surface charges of lauric-acid-capped $CoFe_2O_4$ in water which were characterized by the zeta-potential measurements. As shown in Fig. 3(c), the zeta potential of the bare lauric-acid-capped $CoFe_2O_4$ NPs is -16.2 mV while the zeta-potential values of the CTAB-and SDS-modified lauric-acid-capped $CoFe_2O_4$ NPs are around 34.8 and -26.6 mV, respectively. The high zeta-potential absolute values of $CoFe_2O_4$ NPs in water dispersions indicate their high stability after surfactant modification. The successful surface modification of CTAB and SDS on lauric-acid-capped $CoFe_2O_4$ NPs was confirmed by the FTIR spectra in Fig. 4. For CTAB-modified lauric-acid-capped $CoFe_2O_4$ NPs, the observed band at 603 cm^{-1} as shown in Fig. 4(a) corresponded to the intrinsic stretching vibrations of the metal at the tetrahedral site. The absorption band at 1465 cm^{-1} indicated the existence of–CH_2–group of the CTAB [25], [26]. The FTIR spectrum in Fig. 4(b) confirmed that the $CoFe_2O_4$ NPs were successfully modified with CTAB. The characteristic bands at 989 and 1285 cm^{-1} in the range of 900–1600 cm^{-1}, as shown in Fig. 4(c), are associated with the sulfate group on the SDS surfactant. The absorption band at 1413 cm^{-1} corresponded to the scissoring of methylene group, indicating that the surfactants were successfully modified on the $CoFe_2O_4$ NPs [27], [28].

Magnetic hysteresis loops of both the CTAB-and SDS-modified $CoFe_2O_4$ NPs at room temperature are shown in Fig. 5. The saturation magnetization of the CTAB-and SDS-modified $CoFe_2O_4$ NPs are 38.5 and 33.6 emu $\cdot$ g^{-1}, which are smaller than that of the pure $CoFe_2O_4$ NPs (72 emu $\cdot$ g^{-1}) because of the additional mass of the nonmagnetic surfactants.

C. DOX Loading and Release Test of Surface-Modified Lauric-Acid-Capped $CoFe_2O_4$ Nanoparticles

DOX has been widely used in cancer treatment due to its great clinical effects in chemotherapy, but the dosage administered is strongly limited by their severe side effects [29]. The inverse spinel $CoFe_2O_4$ can efficiently loaded with the anticancer drug DOX by supramolecular π–π stacking interactions [30]. Herein, the loaded DOX on the modified lauric-acid-capped $CoFe_2O_4$ NPs in the PBS solution at

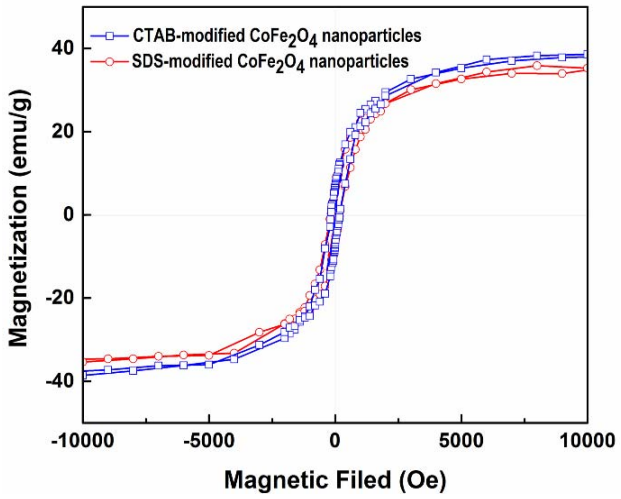

Fig. 5. VSM of CTAB-modified lauric-acid-capped $CoFe_2O_4$ NPs (blue curve) and SDS-modified lauric-acid-capped $CoFe_2O_4$ NPs (red curve).

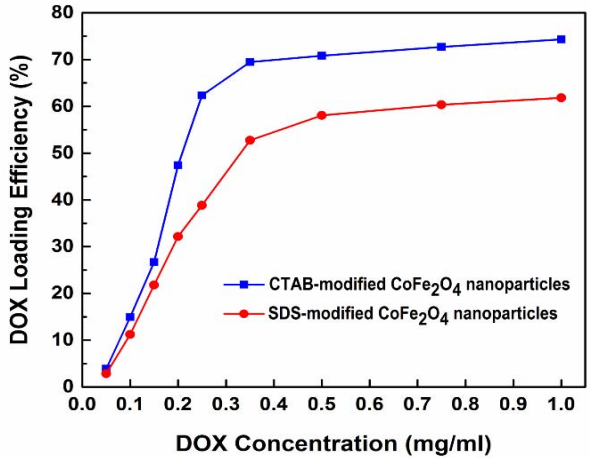

Fig. 6. DOX loading efficiency of CTAB-and SDS-modified lauric-acid-capped $CoFe_2O_4$ NPs.

pH = 7.4 was studied. As shown in Fig. 6, the DOX loading efficiency of the CTAB-and SDS-modified lauric-acid-capped $CoFe_2O_4$ NPs were, respectively, 74.3% and 61.8%. The results confirmed the great drug-loading capacity of modified lauric-acid-capped $CoFe_2O_4$ NPs.

The *in vitro* drug release from the drug-loaded lauric-acid-capped $CoFe_2O_4$ NPs was studied with different pH values (Fig. 7). The results show that the release process of DOX from NPs can be triggered through tuning pH values. When the pH value of PBS solution is 7.4, the DOX on the lauric-acid-capped $CoFe_2O_4$ NPs remained stable; the cumulative DOX released from CTAB-modified and SDS-modified lauric-acid-capped $CoFe_2O_4$ NPs is less than 14% after immersion in PBS for 48 h. On the other hand, the CTAB-modified and SDS-modified lauric-acid-capped $CoFe_2O_4$ NPs exhibited a significant release of DOX when the pH value of solution is 4. The amount of DOX released from the CTAB-modified and SDS-modified lauric-acid-capped $CoFe_2O_4$ NPs increased to 56.1% and 48.2%, respectively; this was attributed to the improvement of water solubility and hydrophilicity of DOX in

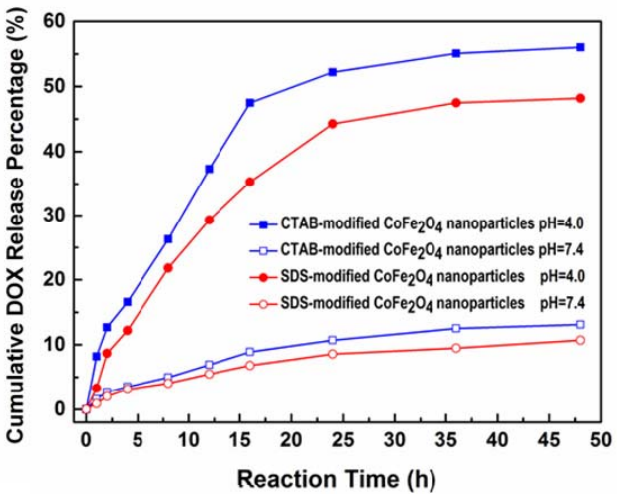

Fig. 7. DOX release curves of CTAB- and SDS-modified lauric-acid-capped $CoFe_2O_4$ NPs at pH = 4 and pH = 7.4.

decreased pH value, which was caused by the increase in protonation of the ammonium groups on DOX [31], [32]. These values are similar to the previous reported results using related nanomaterials [33]. The pH-triggered drug-release mechanism of lauric-acid-capped $CoFe_2O_4$ NPs presents the potential for practical cancer therapy while minimizing the side effects to normal organs by releasing DOX only after entering the acidic microenvironments such as cancerous tissue.

IV. Conclusion

This paper reported a facile one-pot method to synthesize the monodisperse ferrite spinel lauric-acid-capped $CoFe_2O_4$ NPs. The lauric-acid-capped $CoFe_2O_4$ NPs with a particle size of 15.3 ± 1.7 nm were successfully synthesized. The phase transfer of lauric-acid-capped $CoFe_2O_4$ NPs through further surface modification in water with CTAB and SDS was achieved. The surface-modified lauric-acid-capped $CoFe_2O_4$ NPs also possessed high drug loading and excellent pH-responsive drug-release capability. These results reveal that water-soluble lauric-acid-capped $CoFe_2O_4$ NPs can be used as a potential drug delivery system due to its pH-sensitive drug-release properties.

Acknowledgment

This work was supported in part by the Seed Funding Program for Basic Research, the Seed Funding Program for Applied Research, and the Small Project Funding Program from The University of Hong Kong, Hong Kong, in part by RGC-GRF under Grant HKU 17204617, in part by the ITF Tier 3 Funding under Grant ITS-104/13 and Grant ITS-214/14, and in part by the University Grants Committee of HK under Grant AoE/P-04/08.

References

[1] C. Liu, B. Zou, A. J. Rondinone, and Z. J. Zhang, "Chemical control of superparamagnetic properties of magnesium and cobalt spinel ferrite nanoparticles through atomic level magnetic couplings," *J. Amer. Chem. Soc.*, vol. 122, no. 26, pp. 6263–6267, 2000.

[2] K. K. Mohaideen and P. A. Joy, "High magnetostriction and coupling coefficient for sintered cobalt ferrite derived from superparamagnetic nanoparticles," *Appl. Phys. Lett.*, vol. 101, no. 7, pp. 072405-2–072405-6, 2012.

[3] A. J. Rondinone, A. C. S. Samia, and Z. J. Zhang, "Superparamagnetic relaxation and magnetic anisotropy energy distribution in $CoFe_2O_4$ spinel ferrite nanocrystallites," *J. Phys. Chem. B*, vol. 103, no. 33, pp. 6876–6880, 1999.

[4] S. T. Xu, Y. Q. Ma, G. H. Zheng, and Z. X. Dai, "Simultaneous effects of surface spins: Rarely large coercivity, high remanence magnetization and jumps in the hysteresis loops observed in $CoFe_2O_4$ nanoparticles," *Nanoscale*, vol. 7, no. 15, pp. 6520–6526, 2015.

[5] J. Carrey, B. Mehdaoui, and M. Respaud, "Simple models for dynamic hysteresis loop calculations of magnetic single-domain nanoparticles: Application to magnetic hyperthermia optimization," *J. Appl. Phys.*, vol. 109, no. 8, p. 083921, 2011.

[6] U. Häfeli, W. Schütt, J. Teller, and M. Zborowski, *Scientific and Clinical Applications of Magnetic Carriers*. Berlin, Germany: Springer, 2013.

[7] P. Oswald, O. Clement, C. Chambon, E. Schouman-Claeys, and G. Frija, "Liver positive enhancement after injection of superparamagnetic nanoparticles: Respective role of circulating and uptaken particles," *Magn. Reson. Imag.*, vol. 15, no. 9, pp. 1025–1031, 1997.

[8] D. G. Mitchell, "MR imaging contrast agents—What's in a name?" *J. Magn. Reson. Imag.*, vol. 7, no. 1, pp. 1–4, 1997.

[9] M. A. Willard, L. K. Kurihara, E. E. Carpenter, S. Calvin, and V. G. Harris, "Chemically prepared magnetic nanoparticles," *Int. Mater. Rev.*, vol. 49, nos. 3–4, pp. 125–170, 2004.

[10] Z. Xu, C. Shen, Y. Hou, H. Gao, and S. Sun, "Oleylamine as both reducing agent and stabilizer in a facile synthesis of magnetite nanoparticles," *Chem. Mater.*, vol. 21, no. 9, pp. 1778–1780, 2009.

[11] R. T. Olsson, G. Salazar-Alvarez, M. S. Hedenqvist, U. W. Gedde, F. Lindberg, and S. J. Savage, "Controlled synthesis of near-stoichiometric cobalt ferrite nanoparticles," *Chem. Mater.*, vol. 17, no. 20, pp. 5109–5118, 2005.

[12] A. J. Rondinone, A. C. S. Samia, and Z. J. Zhang, "A chemometric approach for predicting the size of magnetic spinel ferrite nanoparticles from the synthesis conditions," *J. Phys. Chem. B*, vol. 104, no. 33, pp. 7919–7922, 2000.

[13] G. V. M. Jacintho, A. G. Brolo, P. Corio, P. A. Z. Suarez, and J. C. Rubim, "Structural investigation of MFe_2O_4 (M = Fe, Co) magnetic fluids," *J. Phys. Chem. C*, vol. 113, no. 18, pp. 7684–7691, 2009.

[14] H. Qu, H. Ma, A. Riviere, W. Zhou, and C. J. O'Connor, "One-pot synthesis in polyamines for preparation of water-soluble magnetite nanoparticles with amine surface reactivity," *J. Mater. Chem.*, vol. 22, no. 8, pp. 3311–3313, 2012.

[15] X. Michalet *et al.*, "Quantum dots for live cells, *in vivo* imaging, and diagnostics," *Science*, vol. 307, no. 5709, pp. 538–544, 2005.

[16] I. L. Medintz, H. T. Uyeda, E. R. Goldman, and H. Mattoussi, "Quantum dot bioconjugates for imaging, labelling and sensing," *Nature Mater.*, vol. 4, no. 6, pp. 435–446, 2005.

[17] Q. Liang, D. Zhao, T. Qian, K. Freeland, and Y. Feng, "Effects of stabilizers and water chemistry on arsenate sorption by polysaccharide-stabilized magnetite nanoparticles," *Ind. Eng. Chem. Res.*, vol. 51, no. 5, pp. 2407–2418, 2012.

[18] A. Swami, A. Kumar, and M. Sastry, "Formation of water-dispersible gold nanoparticles using a technique based on surface-bound interdigitated bilayers," *Langmuir*, vol. 19, no. 4, pp. 1168–1172, 2003.

[19] C. H. Kim *et al.*, "Electronic structure of vertically aligned Mn-doped $CoFe_2O_4$ nanowires and their application as humidity sensors and photodetectors," *J. Phys. Chem. C*, vol. 113, no. 17, pp. 7085–7090, 2009.

[20] J. Li, M. Chen, Z. Gao, J. Du, W. Yang, and M. Yin, "Effective approach towards Si-bilayer-IDA modified $CoFe_2O_4$ magnetic nanoparticles for high efficient protein separation," *Colloids Surf. B, Biointerfaces*, vol. 146, pp. 468–474, Oct. 2016.

[21] D. K. Kim, Y. Zhang, J. Kehr, T. Klason, B. Bjelke, and M. Muhammed, "Characterization and MRI study of surfactant-coated superparamagnetic nanoparticles administered into the rat brain," *J. Magn. Magn. Mater.* vol. 225, nos. 1–2, pp. 256–261, 2001.

[22] S. Sun *et al.*, "Monodisperse MFe_2O_4 (M=Fe, Co, Mn) nanoparticles," *J. Amer. Chem. Soc.*, vol. 126, no. 1, pp. 273–279, 2004.

[23] B. Bateer *et al.*, "Synthesis, size and magnetic properties of controllable $MnFe_2O_4$ nanoparticles with versatile surface functionalities," *Dalton Trans.*, vol. 43, no. 26, pp. 9885–9891, 2014.

[24] B. Debnath, A. Bansal, H. G. Salunke, A. Sadhu, and S. Bhattacharyya, "Enhancement of magnetization through interface exchange interactions of confined NiO nanoparticles within the mesopores of $CoFe_2O_4$," *J. Phys. Chem. C*, vol. 120, no. 10, pp. 5523–5533, 2016.

[25] K. D. Dobson, A. D. Roddick-Lanzilotta, and A. J. McQuillan, "An *in situ* infrared spectroscopic investigation of adsorption of sodium dodecylsulfate and of cetyltrimethylammonium bromide surfactants to TiO_2, ZrO_2, Al_2O_3, and Ta_2O_5 particle films from aqueous solutions," *Vibrational Spectrosc.*, vol. 24, no. 2, pp. 287–295, 2000.

[26] A. Baykal, N. Kasapoğlu, Y. Köseoğlu, M. S. Toprak, and H. Bayrakdar, "CTAB-assisted hydrothermal synthesis of $NiFe_2O_4$ and its magnetic characterization," *J. Alloys Compounds*, vol. 464, nos. 1–2, pp. 514–518, 2008.

[27] M. Singh, H. S. Dosanjh, and H. Singh, "Surface modified spinel cobalt ferrite nanoparticles for cationic dye removal: Kinetics and thermodynamics studies," *J. Water Process Eng.*, vol. 11, pp. 152–161, Jun. 2016.

[28] M. Vadivel, R. R. Babu, M. Arivanandhan, K. Ramamurthi, and Y. Hayakawa, "Role of SDS surfactant concentrations on the structural, morphological, dielectric and magnetic properties of $CoFe_2O_4$ nanoparticles," *RSC Adv.*, vol. 5, no. 34, pp. 27060–27068, 2015.

[29] D. Wang and S. J. Lippard, "Cellular processing of platinum anticancer drugs," *Nature Rev. Drug Discovery*, vol. 4, no. 4, pp. 307–320, 2005.

[30] Z. Liu, X. Sun, N. Nakayama-Ratchford, and H. Dai, "Supramolecular chemistry on water-soluble carbon nanotubes for drug loading and delivery," *ACS Nano*, vol. 1, no. 1, pp. 50–56, 2007.

[31] L. Y. Qiu and M. Q. Yan, "Constructing doxorubicin-loaded polymeric micelles through amphiphilic graft polyphosphazenes containing ethyl tryptophan and PEG segments," *Acta Biomaterialia*, vol. 5, no. 6, pp. 2132–2141, 2009.

[32] F. H. Chen, Q. Gao, and J. Z. Ni, "The grafting and release behavior of doxorubincin from Fe_3O_4 SiO_2 core-shell structure nanoparticles via an acid cleaving amide bond: The potential for magnetic targeting drug delivery," *Nanotechnology*, vol. 19, no. 16, p. 165103, 2008.

[33] G. Wang, Y. Ma, Z. Wei, and M. Qi, "Development of multifunctional cobalt ferrite/graphene oxide nanocomposites for magnetic resonance imaging and controlled drug delivery," *Chem. Eng. J.*, vol. 289, pp. 150–160, Apr. 2016.